Supporting Information

Synthesis of Water-Dispersible Mn^{2+} Functionalized Silicon Nanoparticles under Room Temperature and Atmospheric Pressure for Fluorescence and Magnetic Resonance Dual-Modality Imaging

Ya-Kun Dou,[†] Yang Chen,[‡] Xi-Wen He,[†] Wen-You Li,*[,†,§] Yu-Hao Li,*[,‡] and Yu-Kui Zhang[†,∥]

[†]College of Chemistry, Research Center for Analytical Sciences, State Key Laboratory of Medicinal Chemical Biology, Tianjin Key Laboratory of Biosensing and Molecular Recognition, Nankai University, Tianjin 300071, China, wyli@nankai.edu.cn., Fax: +86-22-23502458

[‡]Key Laboratory of Tumor Microenvironment and Neurovascular Regulation, Nankai University School of Medicine, Tianjin 300071, China, liyuhao@nankai.edu.cn., Fax: +86-22-23502554

[§]Collaborative Innovation Center of Chemical Science and Engineering (Tianjin), Tianjin 300071, China

[∥]National Chromatographic Research and Analysis Center, Dalian Institute of Chemical Physics, Chinese Academy of Sciences, Dalian 116023, China

Table of Contents

Experimental Section

Chemicals and Reagents. All chemicals were analytical grade and used without additional purification. N-(2-Ainoethyl)-3-aminopropyltriethoxysilane (N-APTES, 98%) was purchased from Adamas Reagent Co., Ltd. Ethylenediaminetetraacetic acid manganese disodium salt hydrate (EDTA-$MnNa_2$) was gained from Alfa (USA). N-(3-Dimethylaminopropyl)-N-ethylcarbodiimide hydrochloride (EDC, 98%) and N-hydroxysuccinimide (NHS, 98%) were obtained from HEOWNS (Tianjin, China). (+)-Sodium L-ascorbate (AS, 99%), hydrochloric acid (HCl), sodium hydroxide (NaOH), fluorescein isothiocyanate (FITC) were purchased from J&K Scientific Ltd (Beijing, China). Ultrapure water (Aquapro, 18.25 MΩ·cm) was applied to dilute the solution throughout. A549 human lung carcinoma cells were maintained in Roswell Park Memorial Institute 1640 medium (RPMI-1640; Biological Industries, Israel) containing 10% (v/v) fetal bovine serum (FBS; BI, Israel) and 1% penicillin-streptomycin solution (PS; Thermo Scientific, DE, USA). Wild-type zebrafish embryos (TU strain) were used in this study and raised at 28.5 °C with a 10/14-hour dark/light cycle.[1] Embryos were collected after natural spawning, sorted to remove feces and unfertilized eggs, incubated in E3 medium (5 mmol/L NaCl, 0.33 mmol/L $CaCl_2$, 0.33 mmol/L $MgSO_4$, 0.17 mmol/L KCl, pH 7.2), and developmentally staged by hours post fertilization (hpf). BALB/c nude mice were obtained from Beijing Vital River Laboratory Animal Technology Co., Ltd. All the procedures involving animals were approved by the Institutional Animal Care Committee of Nankai University and conformed to the National Institutes of Health guidelines.

Instrumentations. Transmission electron microscopy (TEM) and high resolution transmission electron microscopy (HRTEM) images were obtained on a Tecnai G^2 F20 transmission electron microscope at an accelerating voltage of 200 kV (FEI, The Netherlands). A nanoparticle analyzer Nano-ZS instrument (Malvern, Britain) was used to obtain the dynamic light scatter (DLS) data and the zeta potential. Fourier transform infrared spectroscopy (FTIR) spectrum (4000-400 cm^{-1}) was obtained on a

Vector 22 FTIR spectrophotometer (Bruker, Germany). X-ray photoelectron spectrometry (XPS) data were measured by an Axis Ultra DLD spectrometer equipped with a mono chromatic Al Ka X-ray source ($h\nu$=1486.6 eV), hybrid (magnetic/electrostatic) optics and a multichannel plate and delay line detector (Kratos Analytical Co., UK). Inductive coupled plasma atomic emission spectrometer (ICP-AES) (Thermo, USA) was applied to measure the content of the silicon and manganese elements in Mn-Si NPs. UV-visible (UV-vis) absorption spectrum of samples was recorded on a UV-2450 spectrophotometer (Shimadzu, Japan). A fluorescence spectrophotometer (F-4500, Hitachi, Japan) was used to obtain the photoluminescence (PL) spectra of samples. The fluorescence lifetime decay curve of Mn-Si NPs was measured by an FLS-920 spectrophotometer (Edinburgh, UK) under 405nm excitation. The magnetic resonance imaging *in vitro* and *in vivo* were carried out with a 1.2 T MRI system (Huantong Corporation, Shanghai, China).

Quantum Yield and Fluorescence Lifetime of Mn-Si NPs. The quantum yields of Mn-Si NPs was calculated *via* a relative method,[2] in which quinine sulfate dissolved in 0.1 M H_2SO_4 (with the known quantum yield of 0.54 at 360 nm) was chosen as a reference. The quantum yield was calculated with the following equation:

$$\Phi_x = \Phi_s (K_x/K_s)(\eta_x/\eta_s)^2$$

Φ_x and Φ_s respectively stand for the quantum yield of Mn-Si NPs and quinine sulfate, K_x and K_s are respectively the slope of curves of Mn-Si NPs and quinine sulfate, and η_x (1.33) and η_s (1.33) stand for the refractive index of Mn-Si NPs and quinine sulfate, respectively. In order to make the results more accurate, all absorption was maintained below 0.05 at the excitation wavelength of 360 nm.

Fluorescence Lifetime decay curve of Mn-Si NPs was measured by an FLS-920 spectrophotometer (Edinburgh, UK) under 405nm excitation.

pH Stability and the Salt Effect of Mn-Si NPs. HCl and NaOH were used to adjust the pH values of Mn-Si NPs' 10 mM phosphate buffer aqueous solution from 3 to 11 to monitor the pH effects on emission stability of Mn-Si NPs. We measured the fluorescence intensities of Mn-Si NPs with different pH values at the same

concentration. The same volume of Mn-Si NPs solution was added to different concentrations (5, 10, 25, 50, 100 mM) of NaCl solution to test the salt effects on emission stability of Mn-Si NPs.

Cytotoxicity Assay. A549 cells were seeded in 96-well plates at 4×10^3 cells/well in 100 μL RPMI-1640 or RPMI-1640 containing Mn-Si NPs (200, 300 and 500 μg/mL) for 3 h, 12 h and 24 h, respectively. *In vitro* cytotoxicity assay was performed with MTT kit (Keygen Biotech, Jiangsu, China) according to the manufacturer's instructions. Three parallel replicates were measured for each sample. The absorbance (OD value) at the wavelength of 550 nm was measured for calculating the cell survival rate using a microplate reader (Promega, WI, USA).

***In vitro* Bioimaging of Mn-Si NPs.** 5×10^4 A549 cells were seeded into 24-well plates with 500 μL RPMI-1640 per well and cultured at 37 °C with 5 % CO_2 for 24 h. To evaluate the bioimaging at different concentrations, cells were then maintained with fresh RPMI-1640 containing Mn-Si NPs at 500, 300, 200 and 150 μg/mL for 12 h, respectively. For time lapse bioimaging, cells were incubated with fresh RPMI-1640 containing Mn-Si NPs at a concentration of 500 μg/mL for 1 h, 3 h, 6 h and 12 h, respectively. Mn-Si NPs-free cells were acted as the control groups. In both assays, the cells were counterstained with 4',6-diamidino-2-phenylindole (DAPI, diluted at 1:1000; Sigma) after washed with 0.1 mol/L phosphate buffer saline (PBS, pH 7.2) and fixed with 4% paraformaldehyde (PFA) in the dark, then sealed the cells on the glass slides with mounting medium (KDL, MA, USA). Confocal fluorescence images were pictured by an FV 1000 confocal microscope (Olympus, Japan). The green fluorescence pictures of Mn-Si NPs were acquired under the 488nm excitation light. The blue fluorescence pictures of nuclei stained with DAPI were captured under the 405nm excitation light, and the emission wavelength were 425-475 nm and 500-600 nm, respectively.

Aqueous Exposure and *In vivo* Bioimaging on Zebrafish. Mn-Si NPs aqueous exposed zebrafish experiment was carried out in line with Organization for Economic Co-operation and Development (OECD) Guidelines.[3] 50 embryos per group removing

dead embryos, at one- to four-cell stage, were placed into 24-well plates and soaked with Mn-Si NPs-E3 medium. The embryos were exposed with E3 medium containing Mn-Si NPs of 200, 100, 50, 25 μg/mL in the dark for three hours. The identical numbers of embryos were cultured only in E3 medium as a control. The embryos were returned to E3 medium and raised regularly after removing Mn-Si NPs. To evaluate the toxicity of Mn-Si NPs, the survival rate and hatching rate of the embryos were monitored at 0, 12, 24, 36 hpf and 48, 60, 72 hpf, respectively. For *in vivo* fluorescence bioimaging, one- to four-cell stage embryos were exposed to Mn-Si NPs-E3 medium at concentrations of 200, 100, 50, and 25 μg/mL for three hours and returned to E3 medium until 12 hpf. Embryos were then grown in E3 medium that contains 0.003% 1-phenyl-2-thiourea (PTU; Sigma) to block pigmentation and mediate observation. The aqueous exposure experiment described above was repeated 3 times.

Statistical Analysis. GraphPad Prism Software (version 6.0; GraphPad, CA, USA) was used to perform the statistical analysis. The viability of A549 cells, the survival rate and hatching rate of zebrafish embryos were presented as the percentage (means ± SD) from 3 repeated experiments. The comparison among groups was based on one-way analysis of variance (ANOVA). A P value of 0.05 was set as the level for statistical significance.

***In vitro* and *In vivo* MRI.** *In vitro* T_1-weighted MR images were obtained on a 1.2 T MRI system (Huantong Corporation, Shanghai, China). The parameters settings were as follows: TR/TE = 100.0/8.8 ms, slice thickness = 1 mm, 30.0 ℃. The relaxation time values (T_1) of Mn-Si NPs solution with different Mn^{2+} concentrations were measured on the same MRI system (1.2 T). Take $1/T_1$ as the ordinate and Mn^{2+} concentration (mM) as the horizontal coordinate to obtain a curve and the slope of the curve was the r_1 relaxivity value of Mn-Si NPs.

A 1.2 T MRI system (Huantong Corporation, Shanghai, China) was used to perform *in vivo* MRI of zebrafish embryos and BALB/c nude mice (13−15 g). The zebrafish embryos were soaked into 24-well culture plates (about 10 embryos per well) with E3

medium at 28.5 °C. Different concentrations of 0, 0.12, 0.23, 0.45, 0.90, and 1.82 mM of Mn^{2+} in Mn-Si NPs were added to the wells, respectively. After being cultured for 4 h, embryos were rinsed with E3 medium three times to remove excess Mn-Si NPs. The washed embryos were packed into transparent pointed centrifuge tube, and then placed in the MRI system to obtain the images. As for MRI in mice, the Mn-Si NPs solution (25 μmol Mn^{2+} per kg) was injected *via* tail vein into the narcotic BALB/c nude mice with 4% chloral hydrate. The anesthetized mice were then placed in the MRI system to obtain the images before injection and after 30 minutes of injection. The MRI parameters were as follows: spin-echo T_1-weighted MRI sequence, TR/TE = 100.0/8.8 ms, FOV = 100 × 50 mm^2, matrix = 256 × 256, slice thickness = 1 mm, 30.0 °C.

***In vivo* Toxicity of Mn-Si NPs in Mice.** The hematoxylin and eosin stained images of main organs (heart, liver, spleen, lung, and kidney) from the control group mice (injected with normal saline) and treatment group mice (injected with Mn-Si NPs) after 7 days of culture were obtained. These organs were soaked in 10% formalin solution for more than 12 h, and then stained with hematoxylin and eosin (H&E) to obtain H&E images, which were applied to discuss the difference between control group and treatment group. Regular statistics of the body weight of mice in control group (injected with normal saline, n=3) and experimental group (injected with Mn-Si NPs, n=3) were carried out to investigate the weight change trend in the two groups.

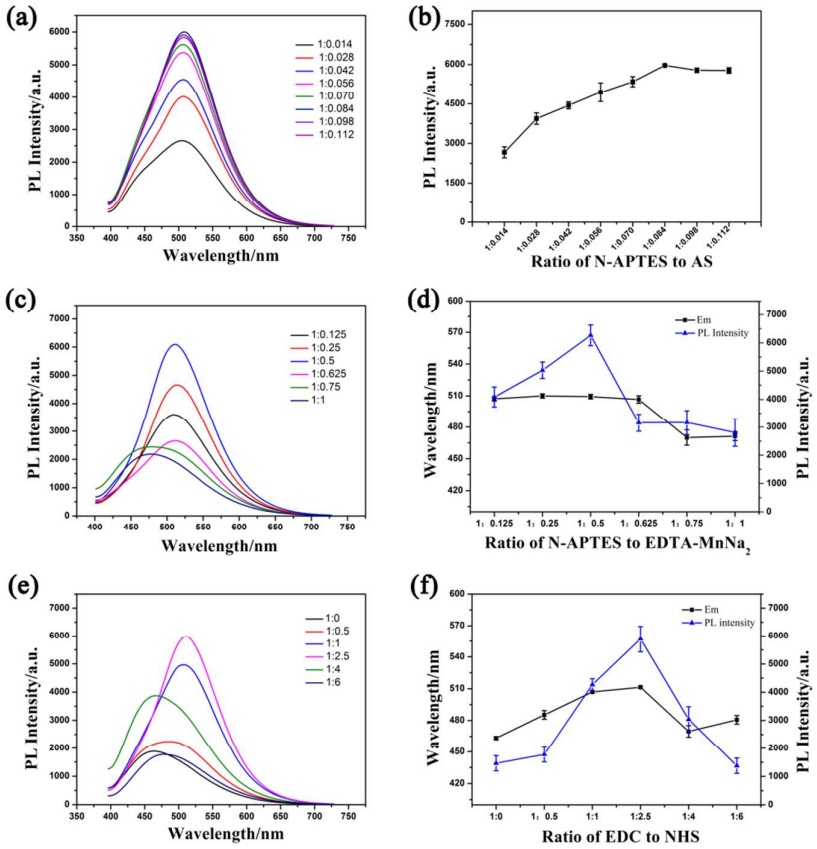

Figure S1. The optimization of synthetic reaction conditions. (a, b) The molar ratio of N-APTES to AS. (c, d) The molar ratio of N-APTES to EDTA-$MnNa_2$. (e, f) The molar ratio of EDC to NHS.

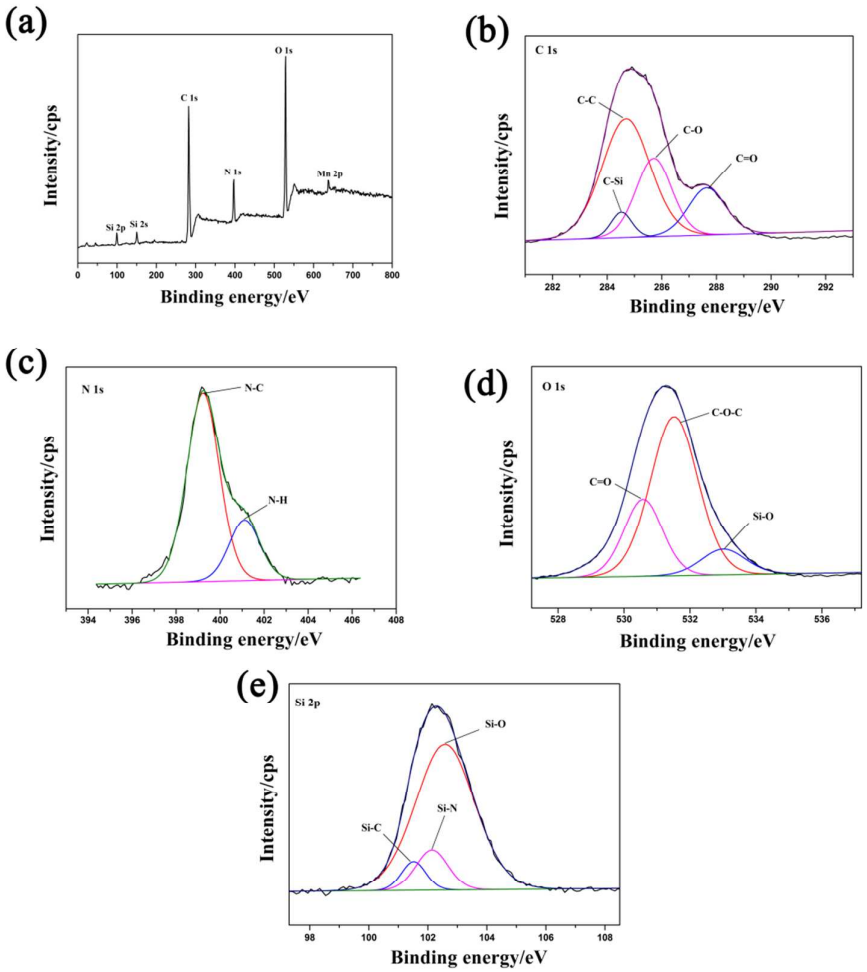

Figure S2. High resolution XPS spectra of (a) full range, (b) C 1s, (c) N 1s, (d) O 1s and (e) Si 2p peak of Mn-Si NPs.

The full range XPS analysis (Figure S2a) of Mn-Si NPs clearly showed five peaks at 99.4, 150.9, 282.1, 397.4, and 529.4 eV, which were attributed to Si 2p, Si 2s, C 1s, N 1s, and O 1s, respectively. [4,5] The C 1s spectrum (Figure S2b) manifested the following five types of carbon atoms: the fitted signals at approximately 284.3, 284.7, 285.7 and 287.6 eV implied the presence of C−Si, C−C, C−O, and C=O. The high-resolution N 1s analysis revealed the peaks at 399.0 and 401.1 eV were for N−C and N−H (Figure S2c).[6–8] This indicated that the as-prepared Mn-Si NPs were rich in amino groups on the surfaces, which was consistent with the corresponding FTIR spectrum. The three fitted peaks at 530.6, 531.5, and 533.0 eV in the O 1s spectra

(Figure S2d) were assigned to C=O, C−O−C, and Si−O groups, respectively.[5, 8] The Si 2p peaks at 101.4, 102.0, and 102.5 eV in Figure S2e could be ascribed to Si−C, Si−N, and Si−O bonds, respectively.[9]

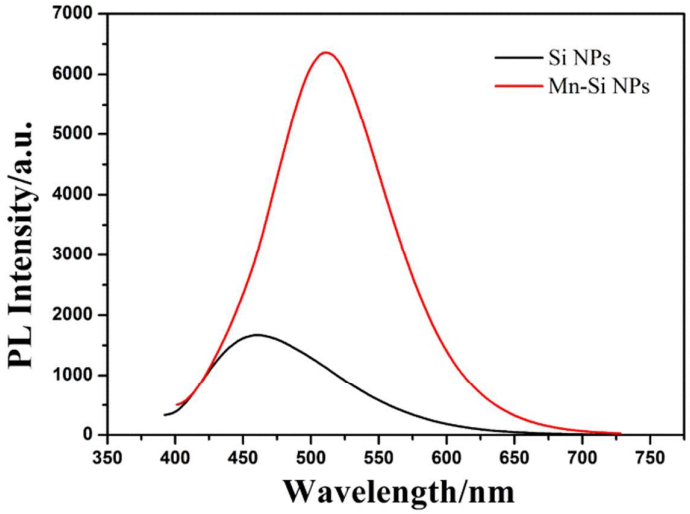

Figure S3. Comparison of luminescence before and after coupling of silicon nanoparticles.

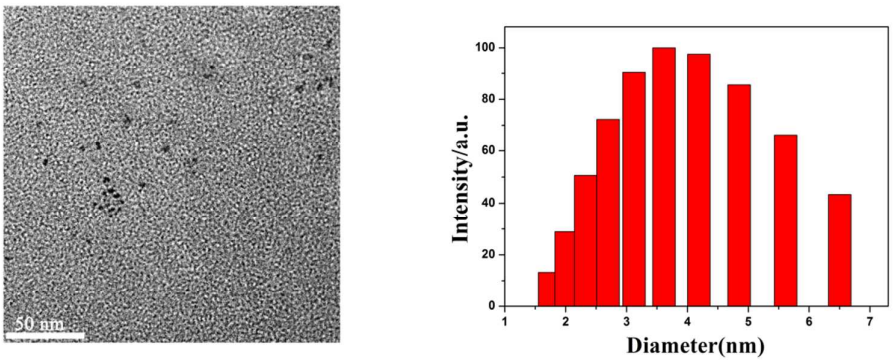

Figure S4. The structure characterizations of Si NPs. (a) TEM. (b) DLS.

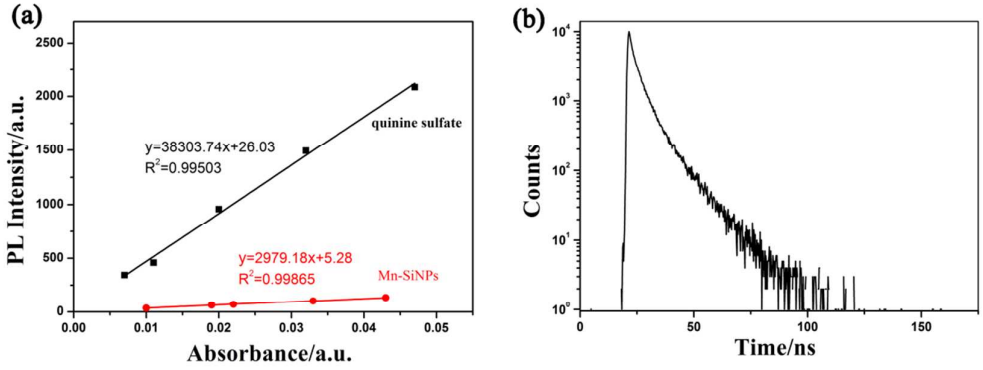

Figure S5. (a) The linear fluorescence-absorbance dependent curves of quinine sulfate and Mn-Si NPs. (b) The fluorescence lifetime spectrum of Mn-Si NPs.

Table S1. Fluorescence lifetime value and relative content of Mn-Si NPs.

Parameter	Value/ns	Relative %
τ_1	2.67	54.34
τ_2	9.38	45.66

$$\tau=2.67*54.34\%+9.38*45.66\%=5.73ns$$

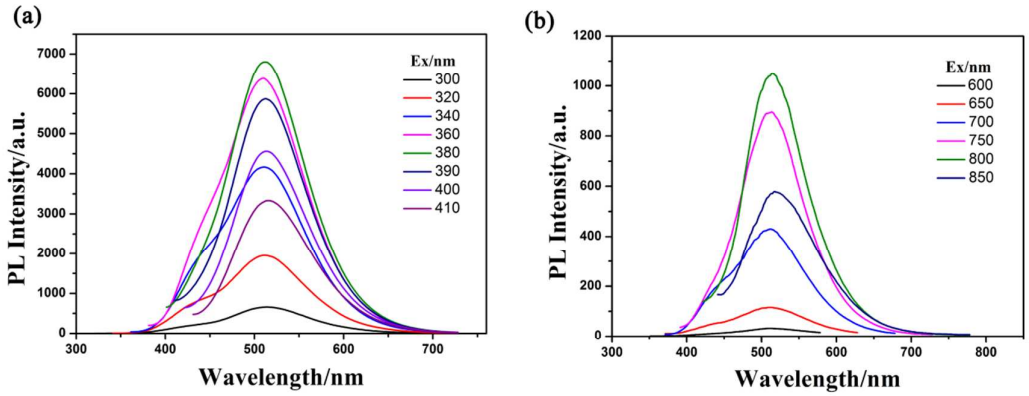

Figure S6. The optical properties of Mn-Si NPs aqueous solution. (a) The excitation wavelength-independent emission spectra with the excitation wavelength varied from 300 to 410 nm. (b) Up-conversion fluorescence spectra with the excitation wavelength changed from 600 to 850 nm.

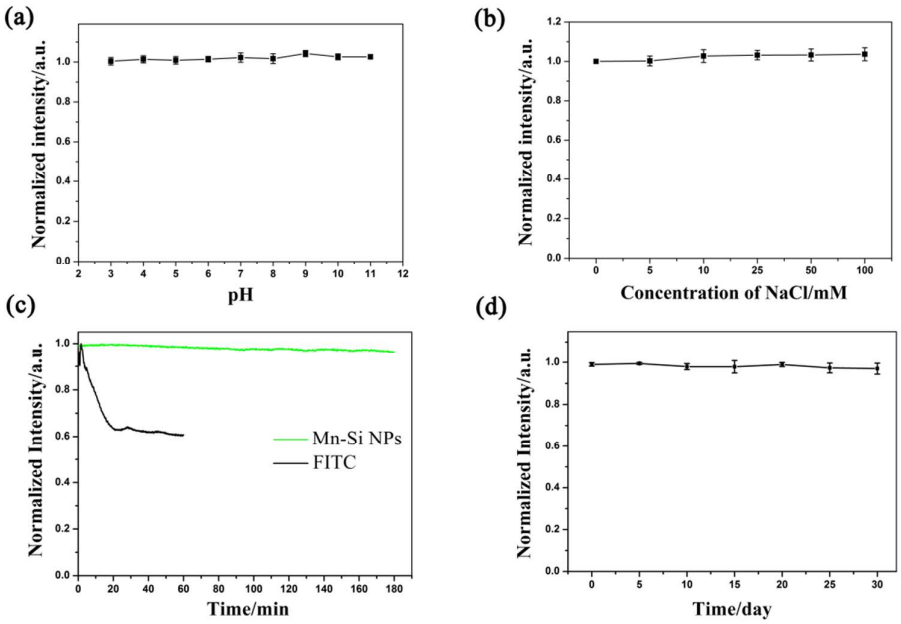

Figure S7. The chemical stability of Mn-Si NPs. (a) pH stability. (b) The salt stability. (c) The photostability. (d) Storage stability.

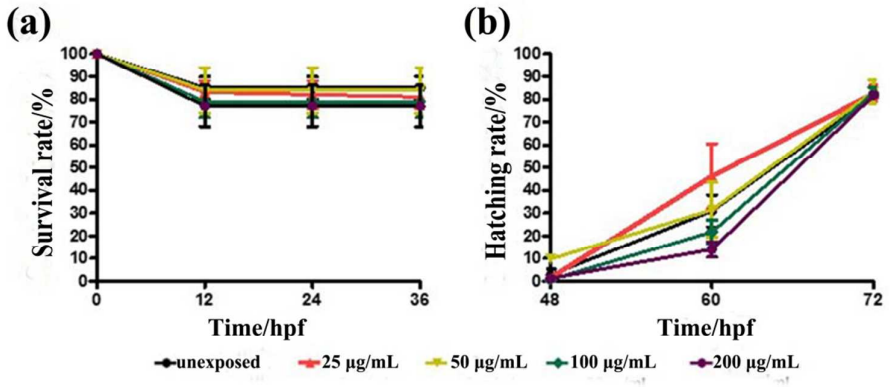

Figure S8. Statistical analysis of (a) the average survival rates and (b) hatching rates of the zebrafish embryos following aqueous exposure to Mn-Si NPs.

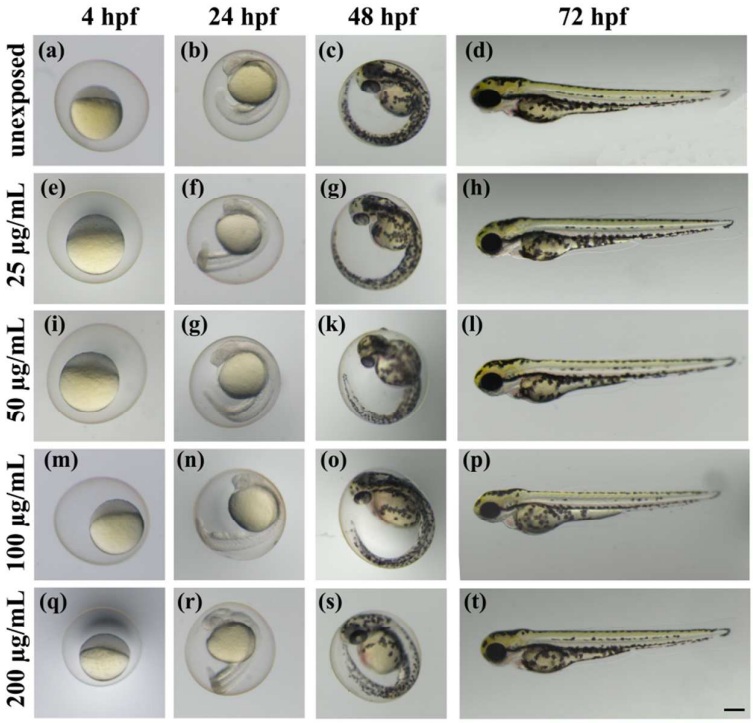

Figure S9. Phenotypes of the zebrafish embryos following aqueous exposure to Mn-Si NPs. Notes: (a-t) Phenotypes of embryos from 4 to 72 hpf in (a-d) the unexposed group and Mn-Si NPs-exposed groups at concentrations of (e-h) 25 μg/mL, (i-l) 50 μg/mL, (m-p) 100 and (q-t) 200 μg/mL. Dorsal is up and rostral is left in (d, h, l, p and t). Scale bar: 200 μm.

References

(1) Westerfield, M. *The Zebrafsh Book : A Guide for the Laboratory Use of Zebrafsh (Brachydanio rerio)*. Eugene: University of Oregon Press, **1993**.

(2) Sankaran, R. M.; Holunga, D.; Flagan, R. C.; Giapis, K. P. *Nano Lett.* **2005**, 5, 537-541.

(3) Buschmann, J. *Methods Mol Biol.* **2013,** 947, 37-56.

(4) Romero, J. J.; Wegmann, M.; Rodríguez, H. B.; Lillo, C.; Rubert, A.; Klein, S.; Kotler, M. L.; Kryschi, C.; Gonzalez, M. C. *J. Phys. Chem. C* **2015**, 119, 5739−5746.

(5) Lillo, C. R.; Romero, J. J.; Portolés, M. L.; Diez, R. P.; Caregnato, P.; Gonzalez, M.

C. *Nano Res.* **2015**, 8, 2047−2062.

(6) Ge, J.; Chen, P.; Jia, Q.; Liu, W.; Zhou, H.; Zhou, B.; Liu, Q.; Wang, P. *RSC Adv*. **2015**, 5, 35291−35296.

(7) Feng, J.; Chen, Y.; Han, Y.; Liu, J.; Ren, C.; Chen, X. *Anal. Chim. Acta*. **2016**, 926, 107-117.

(8) Zhang, H.; Chen, Y.; Liang, M.; Xu, L.; Qi, S.; Chen, H.; Chen, X. *Anal. Chem.* **2014**, 86, 9846−9852.

(9) Wen, G.; Zeng, X.; Wen, X.; Liao, W. *J. Appl. Phys.* **2014,** 115, 164303-164310.